Available online at www.sciencedirect.com
ScienceDirect
Physics Procedia 56 (2014) 184 – 192
Physics Procedia

8th International Conference on Photonic Technologies LANE 2014

Impact of heating rate during exposure of laser molten parts on the processing window of PA12 powder

Dietmar Drummer[a,b], Maximilian Drexler[a,b,*], Katrin Wudy[a,b]

[a]*Collaborative Research Center 814 – Additive Manufacturing (CRC 814), Am Weichselgarten 9, 91058 Erlangen, Germany*
[b]*Institute of Polymer Technology (LKT), Friedrich-Alexander-Universität Erlangen-Nürnberg, Am Weichselgarten 9, 91058 Erlangen, Germany*

Abstract

The additive component manufacturing by selective beam melting of thermoplastic polymer powders can be divided essentially into the following sub-processes: Powder coating, exposure and material consolidation. The mechanical and geometrical properties of a part produced by the selective melting of polymer powders depend to a large extent on these sub-processes. To increase process repeatability basic knowledge about the mutual interactions within the sub-process is of major interest. In the following article the exposure process is focused. Therefore the time dependent energy input into the powder bed is analyzed in its impact on the usable processing window of PA12 powder. Thereby parameters like surface temperature, density and strength of molten layers as well as complex body specimens are quantified for varying exposure heating rates. Therefore methods of statistical design of experiments are used. Due to these investigations the derivation of new, the time dependent material behavior of polymers fitting processing strategies is possible.

Peer-review under responsibility of the Bayerisches Laserzentrum GmbH

Keywords: Selective laser melting; heating rate; part density

1. Motivation and state of the art

Techniques of additive manufacturing are established for prototype construction of special, highly individualized products. This actually changes, as they are now used for a vast number of new application fields. [1-3]

* Maximilian Drexler. Tel.: +49-9131-8529717 ; fax: +49-9131-8529709 .
E-mail address: drexler@lkt.uni-erlangen.de

Peer-review under responsibility of the Bayerisches Laserzentrum GmbH
doi:10.1016/j.phpro.2014.08.162

Especially for technical parts, products made by additive manufacturing processes have increased in importance, now being more than mere demonstration objects [4, 5]. Despite the huge variety of additive manufacturing processes only a few of them have the potential to meet the requirements of flexible industrial series manufacturing of small lot numbers. Considering industrial requirements (e.g. reproducibility of part properties, mechanical strength, contour accuracy) one of the most promising additive processes is the selective laser melting of semi-crystalline thermoplastic powders (Fig. 1). [6]

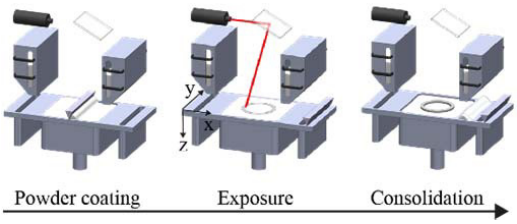

Fig. 1. Selective laser melting process (SLM) of thermoplastic polymer powder.

To achieve industrial standards with beam molten thermoplastic parts exploration of the basic processes is essential. For this purpose the sub-processes (powder coating, exposure, material consolidation) of component generation and their mutual interactions (e.g. melt-pool-dimensions and energy input) are investigated experimentally. Consequently selective laser melting can be investigated in its entirety. Based on this basic research and built on process modeling new adapted process strategies for an improved part quality can be developed. [7, 8]

Currently available processing strategies (e.g. ratio between scanning speed and laser power) are aimed to accelerate the part building process by using higher scanning speeds and laser powers while the volume energy input in a layer is enforced to be kept constant. This evolution bases on the estimation, that equal energy input into the powder bed results in equal melt pool dimensions and part properties. In the following article, the authors will investigate the validity of this estimation. Therefore, within one energy level different exposure speeds are investigated in their effect on the melt pool dimensions as well as part properties. Consequently, effects related to the time dependency of energy input can be faced. For the analysis specimens on different levels of complexity are used, starting with single lines and layers up to whole cubic parts. Due to these investigations effects caused by the energy-input speed can be isolated and new exposure strategies can be derived.

2. Experimental

2.1. Laser-Melting-System (LMS)

To guarantee constant experimental boundary conditions between different experiments, it is necessary to use a special temperature stabilized and homogenized LMS. Due to a multiple heating zone system within the used LMS, the whole building chamber is nearly equally tempered. Consequently disturbing effects caused by temperature variation within the building chamber can be minimized. Moreover a laser system with nearly constant intensity over the whole building chamber is used (F-Theta lens). The scanning system is state of the art and guarantees short acceleration times as well as high precision in beam guiding. The focus diameter d_f is set to 400 µm. Due to the very short exposure times within the design of experiments the heating of the optical gating system is avoided. Consequently the Gaussian beam profile is nearly stable for different exposure parameters.

2.2. Specimens

As specimen rectangular lines are exposed with a CO_2-laser (Fig. 2, left). From the beam diameter d_f and the scanning speed v_s the impact time t can be calculated (equation 1) [9, 10]. Due to the nearly circular shape of beam's cross-section the impact time follows a trigonometric function. Consequently, the time for beam-matter interaction in the edge zones is shorter than for the center line. However, as the beam follows closely a Gaussian distribution and the focus diameter is small compared to scanning speed the resulting error should be relatively small.

$$t = \frac{d_f}{v_s} \tag{1}$$

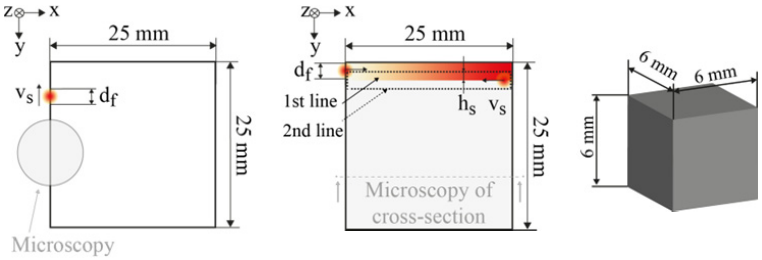

Fig. 2. Single-line specimen (left); single-layer specimen (middle); cubic specimen (right).

With equation 2 the energy input E_{in} during exposure can be approximated based on the laser power P_L.

$$E_{in}(x,y) = P_L(x,y) \cdot t(x,y) = P_L(x,y) \cdot \frac{d(x,y)}{v_s} \tag{2}$$

Based on this approximation and with the assumption of an equilibrium between intrinsic energy and optical energy input (equation 2) with mass m and heat capacity c_p of a penetrated powder-volume element the heating rate H during exposure can be estimated (equation 3).

$$H = \frac{P_L}{m \cdot c_p} = \frac{dT}{dt} \tag{3}$$

Aside from single lines rectangular layers (oriented in their length of the scan paths on the single lines) are molten (Fig. 2, right) at constant building chamber temperature of 172 °C and a hatch distance of h_s=250 µm. Both specimens are exposed without powder coating process. This way, effects caused by the coating process can be excluded.

The production of part-level specimens (cubes and 1:2-scaled tensile bars) is done by using a roller coating system with constant coating parameters (coating speed and amount of coated material), to minimize disturbing effects caused by the coating system [11]. For achieving nearly constant material properties for whole experiments standard laser sintering powder, PA12 (Type: PA2200, EOS GmbH, Krailling, Germany), is used.

The built tensile bars (according to EN ISO 3167, Type A) are scaled with a ratio of 1:2 in size. Due to this scaling the size of the built tensile bars is closer to the size of built single layers. Consequently, disturbing effects caused by varying sizes of specimens are supposed to be diminished. The tensile bars are tested by tensile tests according to DIN EN ISO 527-1, -2. The testing speed is set to 2.5 mm/min. The tensile bars are in ambient humid condition.

2.3. Microscopy

The produced single-line specimens as well as the single layers are analyzed by stereo and transmission light microscopy. The rectangular lines or layers are therefore placed under the microscope and the width of the melting pool d_w as well as the melting depth d_d is measured like shown schematically in Fig. 3.

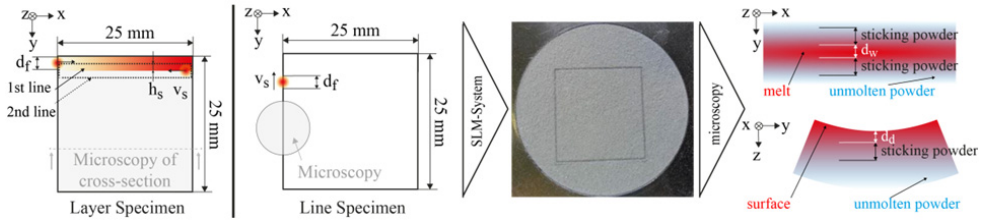

Fig. 3. Microscopic specimen analysis.

For measuring d_w and d_d the exposed specimens are cooled down in the same way and are measured after solidification. To take shrinkage and warpage adequately into account absolute dimension values are not interpreted, they are only compared with specimens measured in the same way.

2.4. Number of defects in molten areas

The percentage of molten areas within a single layer is approximated by counting number of white pixels n_{white} within a transmission light photography in relation to number of black pixels n_{black} of a single layer (Fig. 4). The required threshold for deciding whether a pixel is black or white is kept constant between analyses.

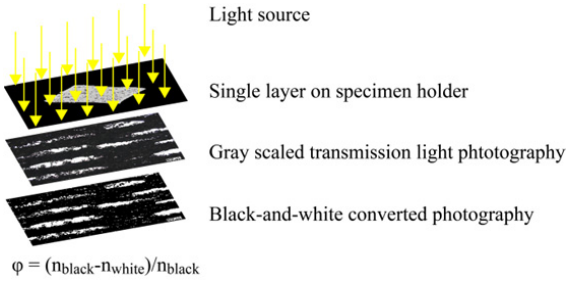

Fig. 4. Transmission light analysis of single-layer specimen.

Effects of layer thickness are neglected by using this kind of optical density analysis of single layers. Consequently, the density of the whole built parts (cubes) is measured. Therefore, the cubes are measured by a caliper (accuracy: ±0.01 mm) and weighed on a precision balance (accuracy: ±0.0001 g). By using the common relation between part's volume and weight the density can be calculated recognizing closed and open pores of the laser molten parts.

2.5. Design of Experiments (DoE)

Table 1 shows the design of experiments. The values for laser power P_L and impact time t are chosen based on industrially used parameters while maintaining a constant energy input during exposure.

Table 1. Design of experiments (DoE).

	Process parameters (E=0.4 J/mm³)		
	Laser-Power P_L	***Heating rate H***	***Scanning speed v_s***
	[W]	***[x10⁷ K/min]***	***[mm/s]***
1	7.8	7.22	780
2	16.0	14.80	1600
3	22.1	20.40	2100
4	27.7	25.62	2770
5	32.9	30.40	3290

3. Results and discussion

3.1. Melt pool dimensions

The melting of polymer powder under exposure of a laser beam is a complex procedure on multiple levels of the material-beam interaction. One resulting quantity of these material-beam interactions is the melt pool and its dimensions. Figure 4 shows the resulting melting widths d_w of single lines for different heating rates.

According to prior investigations [12, 13] increasing the absolute energy input results in a larger melting width d_w. Apart from this trend, a varying relative energy input on a constant energy level also leads to an increasing melting width d_w for higher heating rates (Fig. 5). A reason for this enlargement of d_w might be time dependent effects within the polymer material as well as reduced heat conduction into surrounding powder for shorter impact times. For low heating rates, the absorbed laser power is spread over a large powder volume due to thermal conduction. Consequently, the melting enthalpy needed for this powder volume is not eceeded at any point. Due to this fact for low heating rates only a small melting width d_w is reached next to the point of maximum energy input in the middle of the laser spot. For higher heating rates and along going short impact times the thermal conduction during impact time is tending to be zero. Consequently, the absorbed laser energy is concentrated in a powder volume related to the size of the laser spot. Due to this comperativly small volume, the for melting needed energy is decreased. Based on this estimation the melting width increases for higher heating rates. A hint on a lowered conduction can be seen in the nearly equal overall width of single lines (Fig. 5, pictures). For lower heating rates the amount of unmolten powder sticking to the edges of the specimens is higher than for larger heating rates.

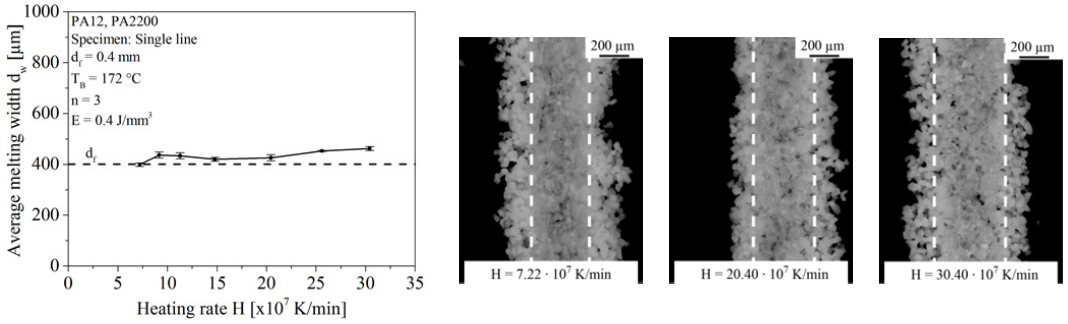

Fig. 5. Width d_w of a molten line for exposure with varying heating rates.

To investigate the layer thickness molten single layers are prepared and measured under microscopy to derive the melting depth d_d. Results are shown in Fig. 6. For small heating rates and along going long impact times absorbed laser energy is conducted over a large powder volume. Consequently, only for portions of conducted volume melting enthalpy is exceeded. For further increased heating rates, heat conduction time is reduced and absorbed laser energy is spread over less powder volume. Due to this fact for melting needed energy decreases and d_d initially increases. It is obvious, that the layer thickness d_d decreases lightly for further rising heating rates. Considering this behaviour higher heating rates seem to favor a heat accumulation next to the exposed surface. Reasonable for this behaviour might be the short impact time combined with high laser power. Due to minimized impact times nearly no time for heat conduction into surrounding powder is possible. Consequently absorbed laser energy is distributed only over directly penetrated particles within the optical penetration depth δ_{opt} (where most of the intensity is extenuated). Due to this fact particles within the penetration-zone are molten. Based on the fact, that thermal conduction into z-direction is minimized for short impact times a heat accumulation next to the exposed surface occurs (compare to chapter 3.2., Fig. 10). Furthermore this heat accumulation next to the surface might result in an increased thermal interaction (e.g. irradiation) between exposed area and building chamber. Consequently, absorbed laser power is lost and melting depth d_d decreases for the higher heating rates. Another hint for estimated heat accumulation can be seen in the temperature measurements (Fig. 10), which are explained in chapter 3.2.

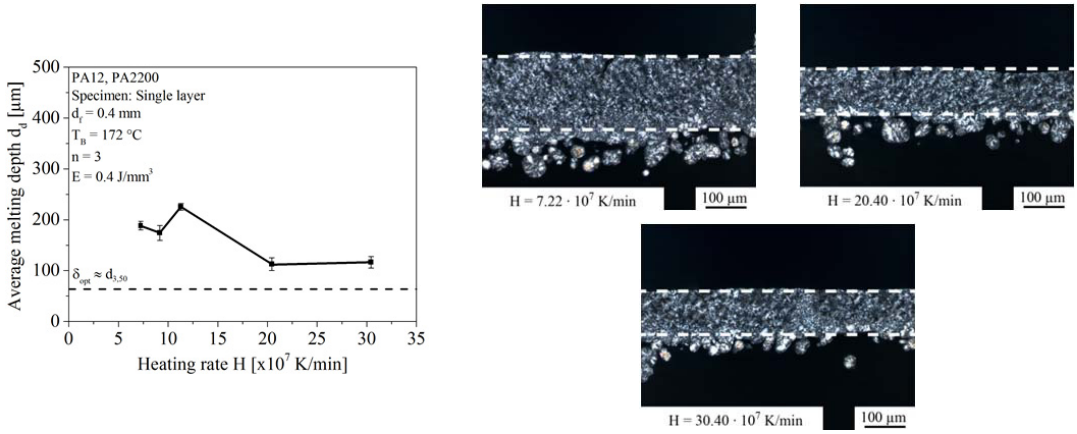

Fig. 6. Thickness d_d of a molten layer for exposure with varying heating rates.

3.2. Resulting processing window

An important characteristic value for the quality of parts produced by beam melting is the part's density. The density correlates directly with mechanical strength of the produced parts, like previous invetigation showed [7, 14]. Due to this fact, the impact of different heating rates on the available processing window of the beam melting process is exemplarily shown on variations in density of the specimens.

Considering the results in Fig. 7 the density of a single layer increases for larger melting width d_w at higher heating rates, while hatching distance h_s kept constant. Fig. 7 shows the optical density of molten single layers analysed by transmission light microscopy. For the investigated design of experiments a high level of layer density appear. Nevertheless for an increasing heating rate within a constant energy level further estimated density increase can be confirmed. During thetransmission light microscopy for density analysis the thickness (z-direction) of the molten layers is neglected. Only the white pixels within the x-y-plane of the layer are counted as holes, which reduce density of the molten layers.

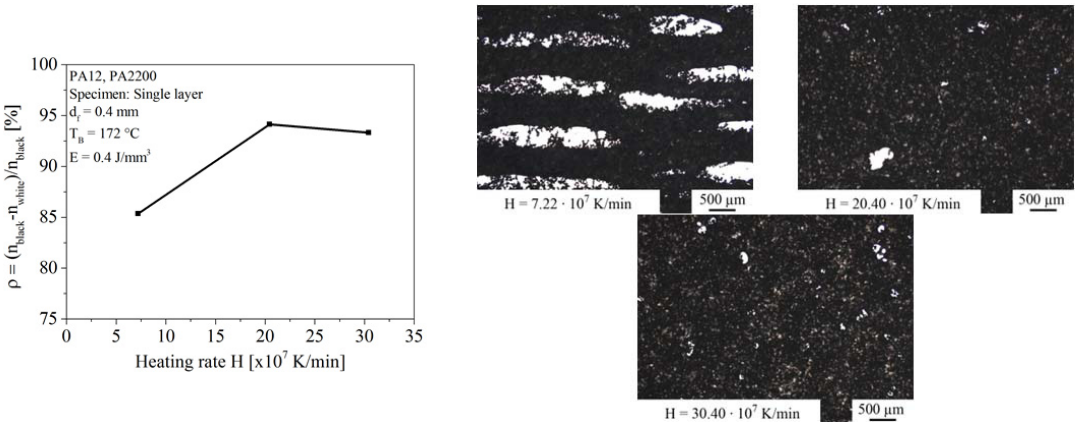

Fig. 7. Optical density of molten areas within a layer for exposure with varying heating rates.

For considering effects on the density of laser molten parts caused by a varying melting depth d_d according to Fig. 6, cubes where built with varying heating rates. Fig. 8 shows the density of the laser molten cubes.

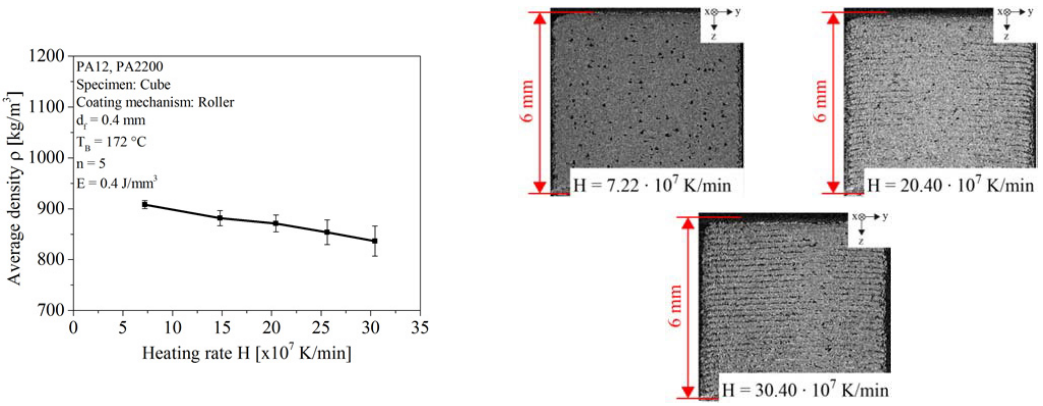

Fig. 8. Density of a molten cube for exposure with varying heating rates and tomographic images (CT) of the samples.

It is obvious, that for an increasing heating rate the density of laser molten cubes declines. Considering the results from Fig. 6 the declining melting depth d_d might be the reason for this effect. Due to the lowered melting depth the connection between the layers of the molten cube is not as strong as for lower heating rates. Consequently, the density of the cubes is reduced. This estimation can be supported by analyzing computer-tomographic pictures, shown in Fig. 8.

Furthermore the estimated decline in part density for increasing heating rates is supported by the results of tensile tests, done with 1:2-scaled (size closer to size of single layers) tensile bars (Fig. 9).

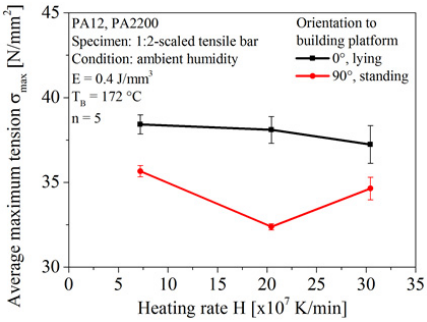

Fig. 9. Tensile tests of 1:2-scaled tensile bars for different orientations to building platform.

For lying as well as standing tensile bars lower maximum tensions appears for increased heating rates. Nevertheless, the tensile tests do not show a clearly visible trend, caused solely by variations in part density. Furthermore effects of density variations are supposed to be superimposed by various effects, e.g. thermal degradation of material or variations in cross-sections size due to heat accumulation during exposure and along going conduction into surrounding powder.

Apart from the reachable density of parts built in x-y-plane as well as for whole parts, the thermal stress of the used polymer is a limiting factor for the processing window. Figure 10 shows the surface temperature for single layers built with varying heating rate.

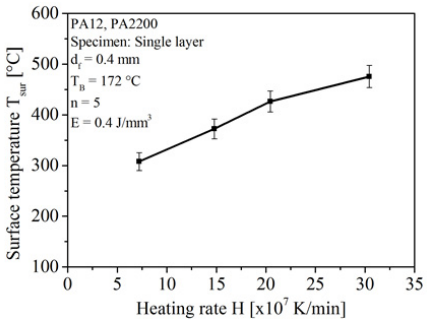

Fig. 10. Surface temperature during exposure of a single layer with varying heating rates.

For an increased heating rate the surface temperature also increases during exposure due to a heat accumulation caused by increasing scanning speed. The reason for the heat accumulation is the shorter time between exposure of single lines of the layer. Consequently, the time for heat transport into the surrounding powder between two exposures declines. Consequently, the surface temperature and along going thermal stress of the polymer increase for higher heating rates. For a degradation temperature of 420 °C (loss of mass 70 %, analyzed by thermogravimetry at 10 K/min) an increased heating rate is believed to lead to thermal degradation of the material (based on the fact, that temperatures > 420 °C are reached for a very short time) within the exposed areas.

4. Conclusion

The authors could show, that the melting width increases for higher heating rates, which causes a denser molten layer in the x-y-plane. In contrast, the melting depth is reduced for higher heating rates, which results in a weaker layer connection. In conclusion it can be summarized, that a varying heating rate influences the usable processing window for generation of PA12 parts. On the one hand, a varying heating rate results in a different melting pool size and along going part densities. On the other hand, the heating rate interacts with the thermal stress of the used polymer. Both factors, melt pool size and surface temperature, are the limiting factors for the usable heating rates. For defining strict limits for heating rates, further investigations are necessary. Especially the time dependent material behavior, e.g. recrystallization effects within the polymer, will be analyzed in future investigations with a special laser differential scanning calorimetry system.

Acknowledgements

The authors want to thank the German Research Foundation (DFG) for funding Collaborative Research Centre 814 (CRC 814), sub-project B03.

References

[1] T. Wohlers: Wohlers Report 2011-State of the industry. 2011.

[2] B. Caulfield, P.E. McHugh, S. Lohfeld: Dependence of mechanical properties of polyamide components on build parameters in the SLS process. In: Journal of Materials Processing Technology 182 (2007), S. 477-488.

[3] J.P. Kruth, B. Vandenbroucke, J. Van Vaerenbergh, P. Mercelis, Benchmarking of different SLS/SLM processes as rapid manufacturing techniques, Int. Conf. Polymers & Moduls Innovations (PMI), Gent, Belgium, 2005.

[4] D. Rietzel, F. Kühnlein, R. Feulner, G. Hülder, C. von Wilmowsky, C. Fruth, E. Nkenke, E. Schmachtenberg, Breaking Material Limitations in Selective Laser Sintering - An Opportunity for Medical Additive Processing, in: S.E.C.o.M. Polymers (Ed.), SPE European Conference on Medical Polymers, Belfast, UK, 2008, pp. 61-65.

[5] W. Hartmann, T. Hausotte, D. Drummer, K. Wudy: Anforderungen und Randbedingungen für den Einsatz optischer Messsysteme zur In-Line-Prüfung additiv gefertigter Bauteile. In: RTejournal - Forum für Rapid Technologie 2012 (2012).

[6] B. Wendel, D. Rietzel, F. Kühnlein, R. Feulner, G. Hülder, E. Schmachtenberg: Additive Processing of Polymers. In: Macromolecular Materials and Engineering 293 (2008), S. 799-809.

[7] D. Rietzel, M. Drexler, F. Kühnlein, D. Drummer, Influence of temperature fields on the processing of polymer powders by means of laser and mask sintering technology, Solid Freeform Fabrication (SFF), Austin, Texas, 2011, pp. 252-262.

[8] D. Rietzel, M. Drexler, D. Drummer, Grundlegende Betrachtungen zur Modellierung transienter thermischer Vorgänge beim selektiven Lasersintern von Thermoplasten, RTejournal - Forum für Rapid Technologie, Erlangen, 2011.

[9] S. Nöken: Technologie des Selektiven Lasersinterns von Thermoplasten. Rheinisch-Westfälische Technische Hochschule Aachen, Fakultät für Maschinenwesen, 1997

[10] B. Keller: Rapid Prototyping: Grundlagen zum selektiven Lasersintern von Polymerpulver. Universität Stuttgart, Institut für Kunststoffprüfung und Kunststoffkunde, Dissertation. 1998

[11] D. Drummer, M. Drexler, F. Kühnlein, Effects on the density distribution of SLS-parts, in: M. Schmidt, F. Vollertsen, M. Geiger (Eds.), Laser Assisted Net Shape Engineering 7 (LANE), Physics Procedia Elsevier B.V. Amsterdam, Fuerth, 2012.

[12] D. Drummer, M. Drexler, K. Wudy, Resulting melt-pool-shape during selective beam melting of thermoplastics as function of energy input parameters, DDMC, Fraunhofer, Berlin, 2014.

[13] D. Drummer, M. Drexler, K. Wudy, F. Kühnlein, Effects of powder bulk density on the prorsity of laser molten thermoplastic parts, 29th International Conference of the Polymer Processing Society, Nuremberg, 2013.

[14] D. Rietzel, F. Kühnlein, D. Drummer: Characterization of New Thermoplastics for Additive Manufacturing by Selective Laser Sintering In: SPE Proceedings ANTEC (2010).